

## Characterization of the bio-oil and bio-char produced by fixed bed pyrolysis of the brown alga *Saccharina japonica*

Jae Hyung Choi\*, Seung-Soo Kim\*\*, Dong Jin Suh\*\*\*, Eun-Jung Jang\*\*\*\*, Kyung-II Min\*\*\*\*, and Hee Chul Woo\*<sup>†</sup>

\*Department of Chemical Engineering, Pukyong National University, 365 Sinseon-ro, Nam-gu, Busan 48513, Korea

\*\*Department of Chemical Engineering, Kangwon National University, 346 Joongang-ro, Samcheok-si, Gangwon-do 25913, Korea

\*\*\*Clean Energy Research Center, Korea Institute of Science and Technology, 5 Hwarang-ro 14-gil, Seongbuk-gu, Seoul 02792, Korea

\*\*\*\*Research Institute of Petroleum Technology, Korea Petroleum Quality & Distribution Authority, 33 Yangcheong 3-gil, Cheongwon-gun, Chungcheongbuk-do 28115, Korea

(Received 12 April 2016 • accepted 5 May 2016)

**Abstract**—Brown alga *Saccharina japonica* was pyrolyzed in a fixed bed reactor under conditions intended to maximize the yield of bio-oil and bio-char. The results revealed that the product distribution of bio-oil, bio-char, and gas was considerably influenced by the pyrolysis temperature (430-530 °C) and holding time (4-10 min). The maximum yields of bio-oil and bio-char were approximately 48.4 and 32.3 wt%, respectively, when prepared at 450 °C for 8 min with a carrier gas flow rate of 2.2 cm/s. The fuel properties of dewatered *S. japonica* bio-oil (DSB) included higher heating value (HHV), kinematic viscosity, density, moisture and ash content, pH, and flash and pour point. The possibility of blending 5-20 vol% DSB with No. 6 fuel oil (Bunker C oil) was also examined. The physicochemical properties of the bio-char exhibited decreased carbon and HHV, and increased inorganic elements and surface area, with increasing pyrolysis temperature.

Keywords: Fixed Bed Pyrolysis, *Saccharina japonica*, Bio-oil, Bio-char, Fuel Property

### INTRODUCTION

Marine macroalgae (i.e., seaweeds) have attracted attention as a potential feedstock for renewable energy because of their short growth cycle, high productivity, high photosynthetic ability, efficient CO<sub>2</sub> fixation, and less competition for food and farmland [1-3]. The macroalgae include members of the brown, red, and green algae, which have been commonly used as ingredients in food, medicine, cosmetics, hydrocolloids, animal feed, and fertilizers [4-6]. The amount of macroalgae cultivated in the world has increased steadily (at a 10% annual growth rate) to reach >15 million wet-metric-tons by 2010 [7]. In particular, two brown algae (*Saccharina japonica* and *Undaria pinnatifida*) are considered the most promising macroalgae species for bioenergy and biorefinery feedstock [3,8,9], and have a much higher uptake of inorganic carbon (e.g., CO<sub>2</sub>, HCO<sub>3</sub><sup>-</sup>, and CO<sub>3</sub><sup>2-</sup>) and higher energy density than any other algae [1].

Brown algae can be converted to biofuels such as bioethanol [10,11], biogas (i.e., methane or hydrogen) [12,13], and bio-oil [14-19] through biological and thermochemical processes. The bio-oil

known as pyrolysis oil can be directly produced by fast pyrolysis, which is rapid thermal decomposition of biomass such as straw, wood, sewage sludge, and micro- and macro-algae, in the absence of oxygen [20,21]. The product is generally a complex dark brown mixture that mainly includes hundreds of oxygenated organic compounds such as aldehydes, alcohols, carboxylic acids, esters, ethers, furans, ketones, phenols, and anhydrosugars [14,20,22]. However, the bio-oil yield and its chemical composition are influenced by the biomass species and pyrolysis conditions such as reactor type, and whether or not catalysts are used.

Fast pyrolysis is known as higher bio-oil yield because the feedstock is rapidly heated in the absence of air [23]. Appropriate reactor types for different biomass species can be selected by examining heat transfer rates, the quenching of the pyrolysis vapors, and the flow rate of the carrier gas [24]. Our previously published work showed that the pyrolysis behavior of *S. japonica* was much different than that of terrestrial biomass [16,17]. Also, the fast pyrolysis of *S. japonica* using a fluidized bed reactor made it difficult to sustain continuous operation because of the formation of sticky products by alginate and minerals in the biomass [19].

In this study, a fixed bed reactor was used for the pyrolysis of *S. japonica* to evaluate the effect of pyrolysis temperature, holding time, and carrier gas flow rate on the yields of bio-oil and bio-char. Pyrolyzed products (bio-oil, bio-char, and gases) were systematically characterized. There is no available information and published literature for the fuel properties, which were derived from biomass

<sup>†</sup>To whom correspondence should be addressed.

E-mail: woohc@pknu.ac.kr

<sup>‡</sup>This article is dedicated to Prof. Seong Ihl Woo on the occasion of his retirement from Korea Institute of Science and Technology (KAIST). Copyright by The Korean Institute of Chemical Engineers.

pyrolysis and its mixtures with petroleum based heavy oil. The analysis of bio-oil and petroleum based heavy oil mixture is the first trial in this work. Analyzed fuel properties are useful in helping to provide for the standards of bio-oil based fuels.

## MATERIALS AND METHODS

### 1. Pyrolysis Procedure

Biomass of the marine brown alga *S. japonica* was collected at Wando Island, Republic of Korea. The fresh feedstock was first dried by sunlight to reach a moisture content of approximately 10-15 wt% and dried at 105 °C for 12 h before use [25]. The feedstock was ground with a knife mill and sieved to obtain particles in the range 3-5 mm.

Pyrolysis of *S. japonica* was carried out in a fixed bed reactor with a cylindrical quartz tube (500 mm long, 24 mm inner diameter) filled with a screen mesh holder (330 mm long, 18 mm outer diameter) containing 30 g of sieved biomass (Fig. 1). Nitrogen was fed at a flow rate of 0.6 L/min to remove air from the reactor before reaction. The pyrolysis vapor leaving the reactor was condensed within a series of three condensers (room temperature, ice water, and liquid nitrogen). The condensed liquids (bio-oils) were collected in a flask while the solid residue (bio-char) remained in the screen mesh holder. The pyrolysis conditions were as follows: temperature 430-530 °C, holding time 4-10 min, carrier gas flow rate 1.5-4.4 cm/s. The bio-char yield, defined as the solid dry weight after reaction $\times$ 100/the feed dry weight, was obtained by weighing the biomass holder before and after pyrolysis. The liquid yield was defined as the collected liquids $\times$ 100/feed dry weight. The gas yield was calculated from the balance of the feed dry weight.

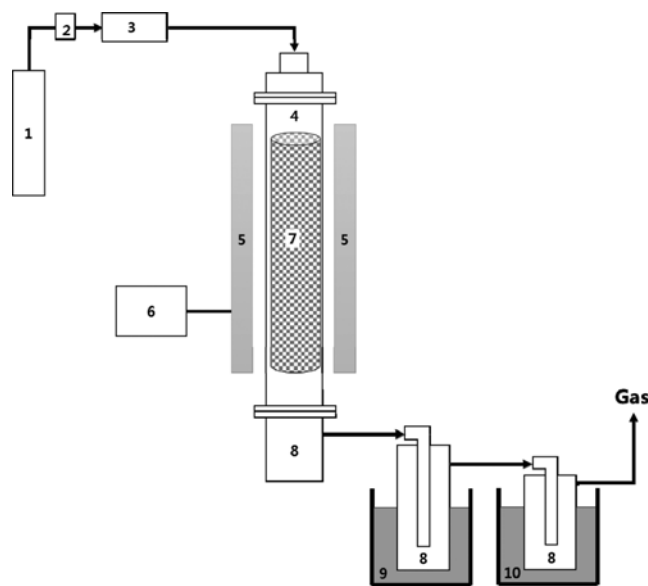


Fig. 1. Schematic diagram of a fixed bed pyrolysis apparatus.

- |                       |                          |
|-----------------------|--------------------------|
| 1. Nitrogen cylinder  | 6. Controller            |
| 2. Valve              | 7. Biomass holder        |
| 3. Flow control valve | 8. Bio-oil storage       |
| 4. Quartz reactor     | 9. Ice bath              |
| 5. Furnace            | 10. Liquid nitrogen bath |

### 2. Preparation of Dewatered Bio-oil Blends

The dewatered bio-oil was prepared using a reduced pressure distillation apparatus. The distillation was in a round-bottom flask with two necks. A distillation column containing ten-theoretical plates, and a receiver connected to a vacuum pump, (N840 Diaphragm Pump, KNE, Germany) were attached to the round-bottom flask. The temperature was monitored by inserting a thermocouple in the distillation tip and a round-bottom flask through the other neck. The distillation of bio-oil for dewatering was carried out according to ASTM standard method D 2892. The dewatered bio-oil was blended with No. 4 fuel oil. A total of 500 mL of blends containing 5, 10, 20 volume percent of the dewatered bio-oil were prepared. The blends for homogenization were stirred at 40 $\pm$ 5 °C for 24 h in 1,000 mL sealed round-bottom flask using a heating mantle.

### 3. Characterization Methods

The proximate analysis of *S. japonica* and bio-chars determined the moisture and ash contents according to ASTM standard methods E 1755 and E 1756. The content of volatile matter was determined using a non-isothermal thermogravimetric (TG) method that follows the ASTM E 872 method. Fixed carbon was calculated from the difference between 100 and the sum of the moisture, ash, and volatile matter. The thermal and combustion characteristics of *S. japonica* and the bio-char were also obtained by the TG method. In the TG method, 20 mg of the sample was heated in a thermogravimetric analyzer (TGA 2000, TA Co.) under a nitrogen or an air flow of 30 mL/min. The temperature was programmed from room temperature to 900 °C at a heating rate of 10.0 °C/min. The elemental composition (C, H, N, and S) of the algae and the bio-char were determined using an elemental analyzer (Vario macro/micro, Elementar) according to ASTM standard method D 5373. The higher heating value (HHV) of the *S. japonica* and the bio-char samples was then estimated by the correlation method of Channiwala and Parikh [26]. The metal composition of *S. japonica* and the bio-char samples was analyzed by using an ICP-OES (Optima 5300DV, Perkin Elmer). The N<sub>2</sub>-adsorption isotherms for the bio-char samples were evaluated at 77 K using a high-speed surface area and pore-size analyzer (Nova 4200e series, Quantachrome). The bio-char samples were degassed in the analyzer for 3 h at 120 °C prior to the N<sub>2</sub> adsorption experiments. The resulting N<sub>2</sub> adsorption data were used to determine the BET-N<sub>2</sub> surface area and total pore-volume.

The hydrogen content in the gas products was analyzed by gas chromatograph (HP-5890 GC, Hewlett Packard Co.) with a thermal conductivity detector (TCD), using a Hayesep DB packed column (SS, 30 ft $\times$ 1/8 in, 80/100 mesh). Carbon dioxide (CO<sub>2</sub>), carbon monoxide (CO), and hydrocarbon gases (C<sub>1</sub>-C<sub>4</sub>) were also measured by gas chromatography (HP-5890 GC, Hewlett Packard Co.) with a flame ionization detector (FID), a methanizer of Ni catalyst, and a Porapak Q packed column (SS, 6 ft $\times$ 1/8 in, 80/100 mesh).

The fuel properties of the dewatered bio-oil and the blended oil samples determined included the moisture content (CA-200, Mitsubishi), density (DMA 4500, Anton Paar), pH (SevenCompact S220, Mettler Toledo), flash point (ATM-7, Tanaka), pour point (MPC-602, Tanaka), ash (Muffle furnace, Fisher Scientific), HHV (6400EF, Paar), and kinematic viscosity (CAV-2100, Cannon Instru-

ment Company). These were determined according to the ASTM standard methods E 203, D 4052, E 70, D 93, D 97, D 482, D 240, and D 445, respectively. The elemental composition (C, H, O, N, and S) of the bio-oil was determined using elemental analyzers (FLASH 2000, Thermo Scientific; FLASH 1112 series, Thermo Finnigan; TN-110, Mitsubishi Chemical Co.; NSX-2100V, Mitsubishi Chemical Analytech) according to the ASTM standard methods of D 5291, D 5622, and D 4294. The solids content in the bio-oil was determined according to the ASTM standard method D 7579. This was accomplished by dissolving a 10 g sample of bio-oil in a 1 : 1 solution of methanol and dichloromethane for 30 min, and then filtering the resulting mixture with a paper filter (0.45  $\mu\text{m}$ ). This was dried in an oven at 60 °C for 24 h prior to the measurement of the remaining weight.

## RESULTS AND DISCUSSION

### 1. Pyrolysis Yields

The results of the proximate and ultimate analysis and heating value of the *S. japonica* sample before pyrolysis in the fixed bed reactor, are summarized in Table 1. The data were compared to those of Bae et al. [16] and Kim et al. [17]. The composition characteristics of *S. japonica* samples produced from South Korea were found to be quite similar. The ash content of *S. japonica* was much higher than that of lignocellulosic biomass (2.7-12.1 wt%) [16,21],

**Table 1. Proximate and ultimate analysis and heating value of *S. japonica* samples**

Parameter	This work	Bae et al. [16]	Kim et al. [17]
Proximate analysis (wt%)			
Moisture <sup>a</sup>	2.79	7.65	6.90
Volatile matter <sup>b</sup>	70.90	53.10	68.79
Fixed carbon <sup>c</sup>	3.32	10.97	4.10
Ash <sup>d</sup>	22.99	28.28	20.21
Ultimate analysis (wt%, dry basis)			
Carbon	42.09	30.60	32.89
Hydrogen	4.38	4.89	6.17
Nitrogen	1.53	1.51	0.93
Sulfur	0.40	0.56	n/a
Oxygen <sup>c</sup>	51.60	62.44	60.01
HHV <sup>e</sup> (MJ/kg)	14.05	6.41	12.11
Metal content (ppm)			
Ca	7,621	7,726	7,002
K	134,063	102,470	64,787
Mg	5,900	5,942	4,781
Na	24,101	26,790	30,836
P	1,855	2,111	1,402

<sup>a</sup>Determined according to the ASTM E 1756 standard method

<sup>b</sup>Determined by thermogravimetric analysis

<sup>c</sup>By difference

<sup>d</sup>Determined according to the ASTM E 1755 standard method

<sup>e</sup>The higher heating value (HHV) was estimated by the correlation of Channiwala and Parikh [26]

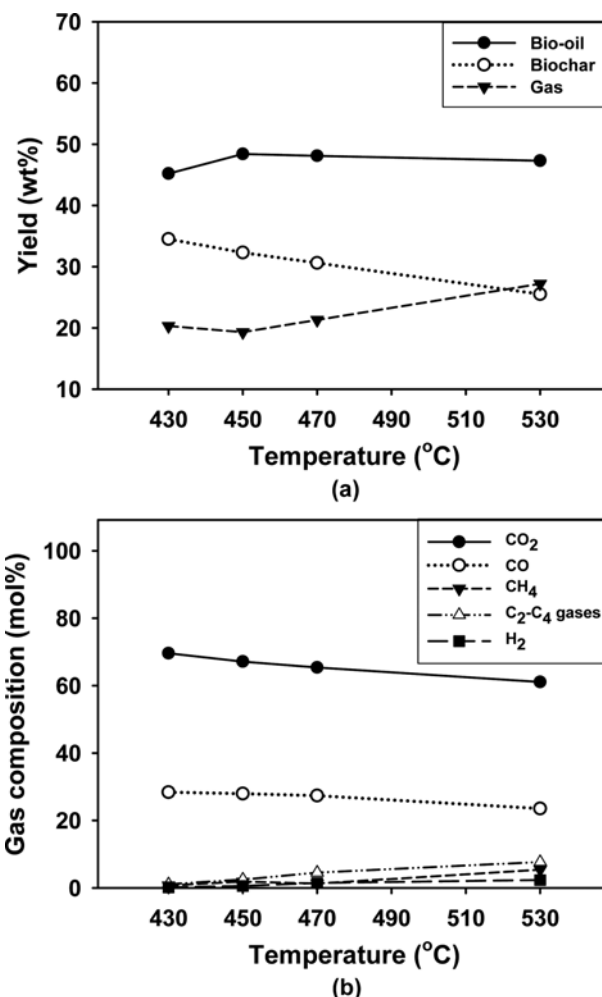


**Fig. 2. Effect of pyrolysis temperature of *S. japonica* biomass on fixed bed pyrolysis: (a) Pyrolysis product yields, (b) pyrolysis gas composition.**

and the alkali and alkaline earth metals (i.e., Ca, K, Mg, and Na) contained in the ash may play a role in catalysis by inhibiting bio-oil production during pyrolysis [14,17,27,28].

The effect of pyrolysis temperature on the product yields is shown in Fig. 2. The product yields of bio-oil, bio-char, and gas were significantly influenced by the temperature within the range 430-530 °C, for holding time of 8 min and carrier gas flow rate of 2.2 cm/s (Fig. 2(a)). The bio-char yield steadily decreased from 34.5 to 25.5 wt%, with rising temperature. This was the opposite of the gas yield, which increased from 20.3 to 27.2 wt%. The yield of bio-oil was maximal at 450 °C (48.4 wt%), and then decreased as the temperature increased. The pyrolysis temperature and heat transfer play an important role in the product distribution [16,23,29]. Compared with packed-tube pyrolysis at the same temperature [16], in a fixed-bed reactor, the pyrolysis of *S. japonica* biomass produced more bio-oil and less bio-char. Generally, a high ash content in the biomass caused lower bio-oil yield [16,17,21]. However, a decrease of bio-oil yield can be prevented by careful selection of the pyrolysis reactor design [21]. The gas products were mainly composed of CO<sub>2</sub>, CO, H<sub>2</sub>, CH<sub>4</sub>, and C<sub>2</sub>-C<sub>3</sub> gases (ethane, ethylene, and propane). The

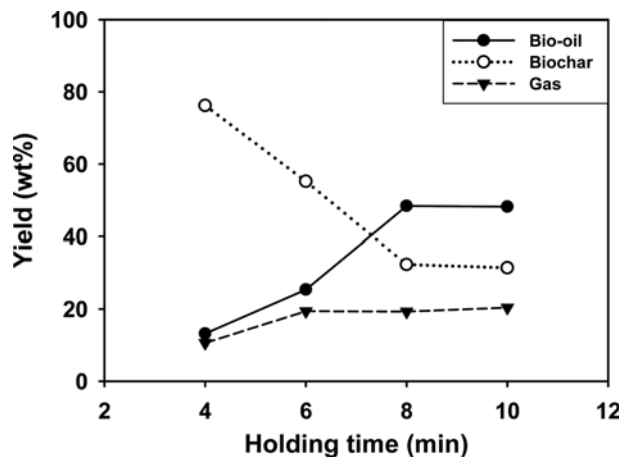


Fig. 3. Effect of holding time of *S. japonica* biomass on fixed bed pyrolysis.

initial main components, CO<sub>2</sub> and CO, steadily decreased with rising temperature, whereas the H<sub>2</sub>, CH<sub>4</sub>, and C<sub>2</sub>-C<sub>4</sub> gases increased due to secondary cracking of substances in the pyrolysis vapor, such as aliphatic and aromatic structures (Fig. 2(b)). This phenomenon was also observed in studies of fast pyrolysis of lignocellulosic and other algal biomass [16,21,30].

The effect of holding time on product yields is shown in Fig. 3. The holding time is the period the biomass remains in the fixed bed reactor. This is a major parameter of heat transfer into the biomass in a pyrolysis reactor. As observed, the bio-char yield markedly decreased with increasing holding time (4-8 min). The maximum yield of bio-oil was reached with a holding time of 8 min at 450 °C under a nitrogen flow of 2.2 cm/s. Meanwhile, the gas yield did not change significantly with change in holding time. This observation indicates that thermo-conversion of the biomass into condensable vapor (bio-oil) is complete at a holding time of 8 min. However, decreasing the holding time leads to incomplete heat transfer results in lowered efficiency of biomass pyrolysis [30].

Pyrolysis vapors generated from the surface of the heated biomass can quickly be swept out by the carrier gas. Accurate control

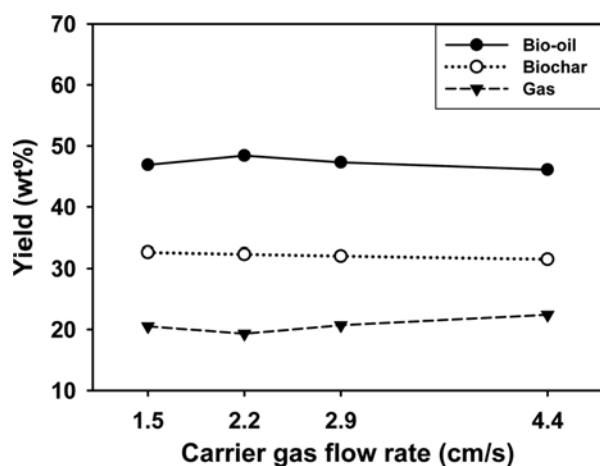


Fig. 4. Effect of carrier gas flow rate of *S. japonica* biomass on fixed bed pyrolysis.

of the carrier gas could provide a positive effect for increasing the yield of bio-oil collected from condensable vapor during pyrolysis. As shown in Fig. 4, the bio-oil yield reached a maximum value of 48.4 wt% when the carrier gas flow rate was 2.2 cm/s (at 450 °C for 8 min), and then decreased as the carrier gas flow rate increased. A slower flow rate (less than 2.2 cm/s) of the carrier gas could cause secondary reactions due to a longer residence time, which most likely would result in the cracking of condensable gas to non-condensable gas, thus increasing the gas yield [31,32]. When the flow is >2.2 cm/s, the higher speed of the carrier gas could cause a loss of condensable gas or entrain fine particles of char into the bio-oil [24]. This observation indicates that the optimal carrier gas flow rate for fixed bed pyrolysis is relatively slower than for fluidized bed pyrolysis [19,33].

## 2. Characterization of Bio-oil

Bio-oils of *S. japonica* were obtained at four different temperatures using the three condensers of the fixed-bed batch system (Fig. 1). As shown in Table 2, the greatest amount of bio-oils was collected at the second condenser, whereas the least amount of bio-oils was collected at the third condenser. A high moisture content (63.2-83.7 wt%) was measured in all the bio-oils at the second and third condensers, whereas a low water content (28.9-33.9 wt%) was measured in the bio-oils collected at the first condenser. All of the bio-oils collected at all of condensers underwent phase separation into dark brown and transparent phases within 24 h. This aging phenomenon is considered due to high moisture content as well as to different polarities of sugars, aliphatics, and aromatics in bio-oil [34,35]. All of bio-oils collected at the first condenser exhibited transparent aqueous and dark oil phases (top and bottom layers, respectively), whereas the bio-oils collected at the second and third condensers exhibited a dark oil top layer and a transparent aqueous bottom layer. Except for the bio-oils collected at the third condenser, the solids suspended in the bio-oils were 0.055-0.968 wt%.

The bio-oil produced by pyrolysis is completely different from petroleum fuels with regard to physical and chemical properties. It is necessary to understand the fuel properties of a bio-oil derived from macroalgae for use in many stationary applications such as

Table 2. Yields and properties of bio-oils at different pyrolysis temperatures

Pyrolysis temperature (°C)	425	450	475	530
Yield (wt%)				
First condenser	13.1	15.4	12.7	11.2
Second condenser	28.3	28.6	29.2	30.5
Third condenser	3.8	4.4	6.2	5.6
Total	45.2	48.4	48.1	47.3
Moisture content (wt%)				
First condenser	28.9	31.4	32.8	33.9
Second condenser	63.2	63.9	65.5	67.6
Third condenser	78.8	81.2	82.5	83.7
Solid content (wt%)				
First condenser	0.968	0.820	0.711	0.556
Second condenser	0.063	0.065	0.591	0.055
Third condenser	0.000	0.000	0.000	0.000

**Table 3. Fuel properties of dewatered *S. japonica* bio-oil (DSB) in comparison with crude bio-oil, ASTM D 7544, and No. 6 fuel oil**

Properties	Methods	DSB <sup>a</sup>	Crude bio-oil <sup>b</sup>	ASTM D 7544 <sup>c</sup> (Grade D)	No. 6 fuel oil <sup>d</sup> (Bunker C oil)
HHV (MJ/kg)	ASTM D 240	28.7	8.7	>15	40
Moisture content (wt%)	ASTM E 203	1.49	70.7	<30	0.1
Kinematic viscosity (mm <sup>2</sup> /s)	ASTM D 445	264 at 50 °C	n/a	<125 at 40 °C	351 at 50 °C
Density (kg/dm <sup>3</sup> )	ASTM D 4052	1.16 at 20 °C	n/a	1.1-1.3 at 20 °C	0.94-0.96 at 15 °C
Ash content (wt%)	ASTM D 482	0.03	n/a	<0.15	0.03
pH	ASTM E 70	5.7	6.9	Report	n/a
Flash point (°C)	ASTM D 93	84.0	n/a	>45	100
Pour point (°C)	ASTM D 97	5.0	n/a	<-9	21
Elemental composition (wt%)					
Carbon	ASTM D 5291	62.8	16.2	n/a	85.6
Hydrogen	ASTM D 5291	8.3	10.2	n/a	10.3
Nitrogen	ASTM D 5291	2.0	<0.3	n/a	0.6
Sulfur	ASTM D 4294	0.2	<0.3	<0.05	2.5
Oxygen	ASTM D 5622	25.6	63.9	n/a	0.6

<sup>a</sup>Dewatering process by reduced pressure distillation at 40 °C and 40 mmHg

<sup>b</sup>Choi et al. [33]

<sup>c</sup>Determined according to the ASTM D 7544 standard method

<sup>d</sup>Chiaramonti et al. [36]

boilers, furnaces, gas turbines, and diesel engines. In this study, *S. japonica* bio-oil was prepared under reaction conditions including pyrolysis temperature 450 °C, holding time 5 min, and carrier gas flow rate 2.2 cm/s. Then the *S. japonica* bio-oil was dewatered by reduced pressure distillation at 40 °C and 40 mmHg (5.3329 kPa). The fuel properties of the dewatered *S. japonica* bio-oil (DSB) sample are summarized in Table 3. With decreasing moisture content of the DSB, the higher heating value (HHV) of DSB was three times that of crude bio-oil [33], whereas it was lower than that of No. 6 fuel oil [36]. High moisture content of bio-oil can lead to serious problems of phase separation and low energy density [34,35,37]. Meanwhile, with decreasing moisture content in the DSB, the physical and chemical properties (viscosity, density, pH, flash and pour point, and elemental compositions) of the bio-oil were improved. The pH of the DSB was 5.7, which was higher than those of bio-oil samples (pH 2.0-3.9) obtained from lignocellulosic biomass [21,35]. This observation implies that a low pH value may be increased by polymerization or condensation reactions with acidic compounds during reduced pressure distillation [38]. The flash and pour point of DSB may be mainly affected by its chemical composition. Especially, the flash point is attributed to small-molecule compounds

such as ketones, furans, and aldehydes; which evaporate around 84 °C. A suitable flash point can make a fuel considerably less dangerous for handling, transport, and storage. The high pour-point value (5 °C) of DSB is generally associated with a high proportion of sugar derivatives (e.g., alginate, mannitol, fucoidan, and laminarin) and polymerized compounds with carboxylic acids, alcohols, and aldehydes [34,39]. These could lead to problems in the design of fuel injectors, pumps, and pipelines [37]. This DSB has much higher oxygen and nitrogen content compared to petroleum-based fuel oil. The high oxygen content (25.6 wt%) could help improve its combustion as heating oil. Meanwhile, the high nitrogen content (2.0 wt%) in the DSB could increase NO<sub>x</sub> emissions.

The results from blending 5-20 vol% DSB with No. 6 fuel oil (Bunker C oil) are shown in Table 4. Blending a small amount of DSB with No. 6 fuel oil could improve the low heating value of DSB. The ignition delay (flash point) and viscosity of the No. 6 fuel oil was reduced in the DSB blend. Moreover, the DSB has a lower sulfur content, and therefore its blending could reduce the sulfur emission of the No. 6 fuel oil. Up to 20% of the DSB addition on the fuel properties of No. 6 fuel oil could improve combustion stability and reduce sulfur emissions for replacing heavy fuel oil in

**Table 4. Fuel properties of No. 6 fuel oil, DSB, and No. 6 fuel oil/DSB blends**

	No. 6 fuel oil <sup>a</sup>	No. 6 fuel oil/DSB blends			DSB
		95/5	90/10	80/20	
Flash point (°C)	85.5	85.0	84.5	84.0	84.0
Kinematic viscosity at 50 °C (mm <sup>2</sup> /s)	284	281	279	276	264
Sulfur (wt%)	3.30	3.14	2.94	3.11	2.93
Moisture content (wt%)	0.10	0.05	0.22	0.39	1.49
Solid content (wt%)	0.055	0.040	0.095	0.195	0.885

<sup>a</sup>No. 6 fuel oil was from the Korea Petroleum Quality & Distribution Authority

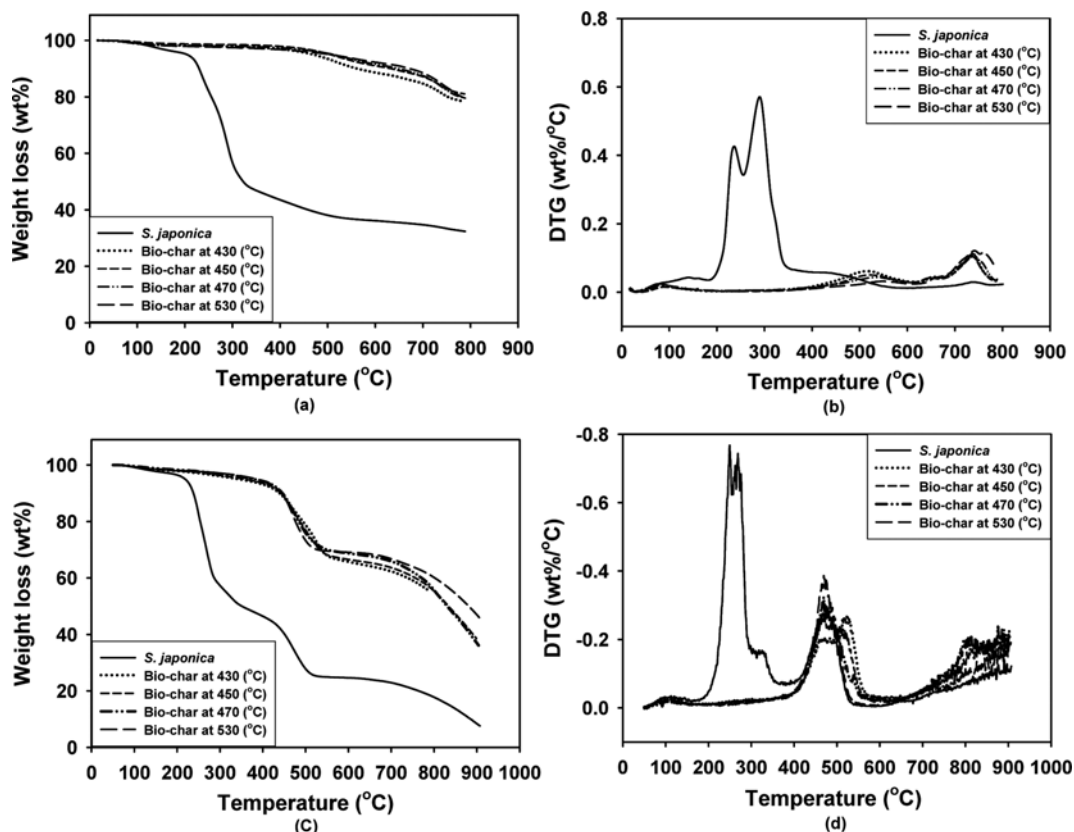


Fig. 5. TG (left) and DTG results (right) of *S. japonica* and bio-char samples at a heating rate of 20 °C/min under nitrogen gas (a), (b) or ambient air (c), (d).

boilers and gas turbines. However, blends of above 20% DSB with No. 6 fuel oil can be immiscible because of high oxygen content (25.6 wt%) of the DSB (Table 3). The DSB could be emulsified with bio-based fuels (e.g., biodiesel and bioethanol) using a surfactant or a solvent, to provide heat and power generation fuels for boilers, furnaces, diesel engines, and gas turbines [35,36].

### 3. Characterization of Bio-char

The pyrolysis behavior of *S. japonica* and the bio-chars according to different pyrolysis temperatures was observed from the TG and differential thermogravimetric (DTG) curves under nitrogen gas (Fig. 5(a) and 5(b)). The thermal degradation of *S. japonica* showed three weight loss steps in the range 200–450 °C. The first and second peaks were at 235 and 290 °C, respectively (Fig. 5(b)), and were associated with the carbohydrate decomposition of alginate, mannitol, fucoidan, and laminarin [14,15,19]. The third peak, from 350 to 450 °C, was associated with the decomposition of protein and lipids [14,16]. The TG curves of the corresponding bio-char were quite similar, indicating further decomposition of bio-char into solid residues, including minerals at temperatures >500 °C.

The combustion behavior of *S. japonica* and the bio-char samples is shown in the burning profiles of TG and DTG curves in ambient air (Fig. 5(c) and 5(d)). These profiles indicate a more complex route compared with the pyrolysis behavior. A stepwise profile of the *S. japonica* sample in the temperature range of 200–400 °C was attributed to the carbohydrates, proteins, and lipids described above. However, similar features were present in the burning pro-

files of the *S. japonica* and bio-chars at temperature >400 °C, and they appeared to have exhibited additional significant weight loss. As reported in previous studies, the presence of alkali metals in the biomass influences the pyrolysis and combustion behavior [14,28,40].

The proximate and ultimate analysis, HHV, bulk density, surface area, and pore volume of the bio-char samples are summarized in Table 5. The ash content steadily increased, whereas the HHV, volatile matter content, and fixed carbon decreased with increasing pyrolysis temperature. As reported in previous studies, the heating value of algae-derived bio-char was typically lower than that of lignocellulosic bio-char due to a comparatively high ash content [14, 21]. The surface area and pore volume of the bio-chars produced at all temperatures were generally low, but the surface area slightly increased from 1.55 to 2.41 m<sup>2</sup>/g, with higher pyrolysis temperature. The surface area and porosity were attributed to the fast release of volatiles during pyrolysis, which produced an open porous structure in the bio-char and minerals [41].

The inorganic elements of the bio-chars can be bound to a carbonaceous matrix. The enrichment ratio of inorganic elements in the bio-char products with different pyrolysis temperatures is shown in Fig. 6. Calcium (Ca), potassium (K), magnesium (Mg), sodium (Na), and phosphorus (P), in order of higher concentration were the major inorganic elements detected (Table 1). The enrichment ratio of inorganic elements (Ca, K, Mg, Na, and P) increased two- to four-times with increased pyrolysis temperature. With the exception of potassium, the inorganic elements increased at a constant

**Table 5. Proximate and ultimate analysis, heating value, surface area, and porosity of bio-char samples**

Parameters	Pyrolysis temperature (°C)			
	430	450	470	530
Proximate analysis (wt%, dry basis)				
Moisture <sup>a</sup>	1.64	1.90	1.29	1.23
Volatile matter <sup>b</sup>	30.35	29.75	29.67	29.06
Fixed carbon <sup>c</sup>	10.64	7.46	6.65	2.01
Ash <sup>d</sup>	57.37	60.89	62.39	67.70
Ultimate analysis (wt%, dry basis)				
Carbon	51.67	47.57	34.70	34.57
Hydrogen	2.54	2.35	1.56	1.86
Nitrogen	1.46	1.75	1.39	1.42
Sulfur	1.54	2.32	1.47	1.14
Oxygen <sup>e</sup>	42.79	46.01	60.88	61.01
O/C molar ratio	0.83	0.97	1.75	1.76
H/C molar ratio	0.05	0.05	0.04	0.05
HHV <sup>e</sup> (MJ/kg)	15.53	13.54	6.47	6.62
Bulk density (g/mL)	0.39	0.40	0.42	0.48
BET surface area (m <sup>2</sup> /g)	1.55	1.88	2.07	2.41
Pore volume (cm <sup>3</sup> /g)	0.0042	0.0058	0.0070	0.0091
Pore size (nm)	18.38	18.05	17.43	17.97

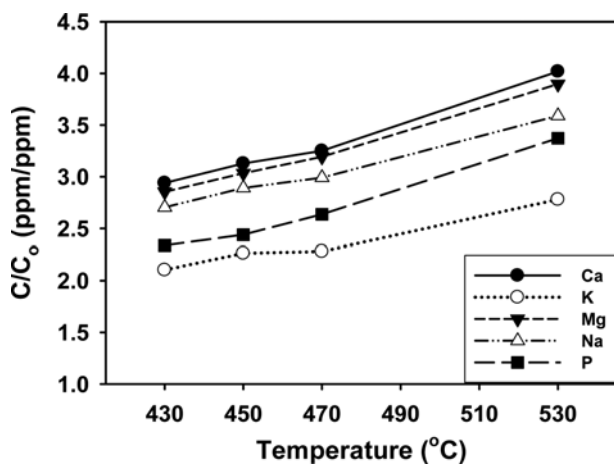
<sup>a</sup>Determined according to the ASTM E 1756 standard method

<sup>b</sup>Determined by thermogravimetric analysis

<sup>c</sup>By difference

<sup>d</sup>Determined according to the ASTM E 1755 standard method

<sup>e</sup>The higher heating value (HHV) was estimated by the correlation of Channiwala and Parikh [26]

**Fig. 6. The enrichment ratio of inorganic elements from bio-chars formed at different pyrolysis temperatures.**

rate. Potassium increased less with higher temperature and may affect different activations (i.e., dehydration, demethoxylation, and secondary reactions) as a catalyst during pyrolysis [14,17,27,28]. Algae-derived bio-chars typically have low carbon content, whereas they have high nitrogen, phosphorus, and alkaline mineral content (e.g., Ca, K, Mg, Na) compared with terrestrial biomass species

[14,41]. The bio-char, with its alkaline carbon materials, could be used to balance acidic soil [42,43] and for long-term carbon sequestration [44].

## CONCLUSIONS

Algal biomass (*S. japonica*) was successfully pyrolyzed using a fixed bed reactor under various conditions to produce a high yield of bio-oil and bio-char. When optimizing the operating conditions of heat and mass transfer, the highest yields of bio-oil (48.4 wt%) and bio-char (32.3 wt%) were achieved at the pyrolysis temperature of 450 °C, the holding time of 8 min, and the carrier gas flow rate of 2.2 cm/s.

To improve the major problem of phase separation of bio-oil caused by its high water content, the crude bio-oil was simply dewatered by reduced pressure distillation at 40 °C and 40 mmHg. The fuel properties of the DSB were improved, including the values of HHV, kinematic viscosity, density, water and ash content, pH, and flash and pour points. For blends of DSB and No. 4 fuel oil, addition of 5-20 vol% DSB could improve the low heating value, ignition delay, high viscosity, and sulfur content of the No. 4 fuel oil. The bio-char derived from *S. japonica* has properties, including comparatively high nutrient content (Ca, K, Mg, N, and P), that make it suitable for use as a soil additive, and for long-term soil carbon sequestration.

## ACKNOWLEDGEMENT

This work was financially supported by the Ministry of Oceans and Fisheries of Korea (Project No. 20140559).

## NOMENCLATURE

ASTM : American society for testing and materials  
 DSB : dewatered *S. japonica* bio-oil  
 DTG : differential thermogravimetric  
 FID : flame ionization detector  
 GC : gas chromatograph  
 HHV : higher heating value  
*S. japonica* : *Saccharina japonica*  
 TCD : thermal conductivity detector  
 TG : thermogravimetric

## REFERENCES

1. K. Gao and K. R. McKinley, *J. Appl. Phycol.*, **6**, 45 (1994).
2. G. Roesijadi, S. B. Jones, L. J. Snowden-Swan and Y. Zhu, *Macroalgae as a biomass feedstock: A preliminary analysis*, Pacific Northwest National Laboratory, Report No.: PNNL-19944, Sponsored by the US Department of Energy (2010).
3. N. Wei, J. Quarterman and Y. S. Jin, *Trends Biotechnol.*, **31**, 70 (2013).
4. H. J. Bixler and H. Porse, *J. Appl. Phycol.*, **23**, 321 (2011).
5. G. Jiao, G. Yu, J. Zhang and H. S. Ewart, *Mar. Drugs*, **9**, 196 (2011).
6. S. Sivagnanam, S. Yin, J. H. Choi, Y. B. Park, H. C. Woo and B. S. Chun, *Mar. Drugs*, **13**, 3422 (2015).
7. FAO Yearbook 2010: Fishery and Aquaculture Statistics, *Food and*

- Agriculture Organization of the United Nations (FAO)*, 2012. [Online]. Available: [ftp://ftp.fao.org/FI/CDrom/CD\\_yearbook\\_2010/booklet/ba0058t.pdf](ftp://ftp.fao.org/FI/CDrom/CD_yearbook_2010/booklet/ba0058t.pdf). [Accessed: 05 January 2015].
8. K. A. Jung, S. R. Lim, Y. Kim and J. M. Park, *Bioresour. Technol.*, **135**, 182 (2013).
  9. M. Song, H. D. Pham, J. Seon and H. C. Woo, *Renew. Sust. Energy Rev.*, **50**, 782 (2015).
  10. A. J. Wargacki, E. Leonard, M. N. Win, D. D. Regitsky, C. N. Santos, P. B. Kim, S. R. Cooper, R. M. Raisner, A. Herman, A. B. Sivitz, A. Lakshmanaswamy, Y. Kashiyama, D. Baker and Y. Yoshikuni, *Science*, **335**, 308 (2012).
  11. M. Enquist-Newman, A. M. E. Faust and D. D. Bravo, *Nature*, **505**, 239 (2014).
  12. T. N. Pham, W. J. Nam, Y. J. Jeon and H. H. Yoon, *Bioresour. Technol.*, **124**, 500 (2012).
  13. M. Song, H. D. Pham, J. Seon and H. C. Woo, *Korean J. Chem. Eng.*, **32**, 567 (2015).
  14. A. B. Ross, J. M. Jones, M. L. Kubacki and T. Bridgeman, *Biore-sour. Technol.*, **99**, 6494 (2008).
  15. K. Anastasakis, A. B. Ross and J. M. Jones, *Fuel*, **90**, 598 (2011).
  16. Y. J. Bae, C. Ryu, J. K. Jeon, J. Park, D. J. Suh, Y. W. Suh, D. Chang and Y. K. Park, *Bioresour. Technol.*, **102**, 3512 (2011).
  17. S. S. Kim, H. V. Ly, G. H. Choi, J. Kim and H. C. Woo, *Bioresour. Technol.*, **123**, 445 (2012).
  18. S. Wang, Q. Wang, X. Jiang, X. Han and H. Ji, *Energy Convers. Manage.*, **68**, 273 (2013).
  19. J. Choi, J. W. Choi, D. J. Suh, J. M. Ha, J. W. Hwang, H. W. Jung, K. Y. Lee and H. C. Woo, *Energy Convers. Manage.*, **86**, 371 (2014).
  20. S. Xiu and A. Shahbazi, *Renew. Sust. Energy Rev.*, **16**, 4406 (2012).
  21. T. N. Trinh, P. A. Jensen, K. Dam-Johansen, N. O. Knudsen, H. R. Sørensen and S. Hvilsted, *Energy Fuels*, **27**, 1399 (2013).
  22. Q. Zhang, J. Chang, T. Wang and Y. Xu, *Energy Convers. Manage.*, **48**, 87 (2007).
  23. G. W. Huber, S. Iborra and A. Corma, *Chem. Rev.*, **106**, 4044 (2006).
  24. A. V. Bridgwater and G. V. C. Peacocke, *Renew. Sust. Energy Rev.*, **4**, 1 (2000).
  25. J. G. Brammer and A. V. Bridgwater, *Renew. Sust. Energy Rev.*, **3**, 243 (1999).
  26. S. A. Channiwala and P. P. Parikh, *Fuel*, **81**, 1051 (2002).
  27. R. Fahmi, A. V. Bridgwater, I. Donnison, N. Yates and J. M. Jones, *Fuel*, **87**, 1230 (2008).
  28. H. Hwang, S. Oh, T. S. Cho, I. G. Choi and J. W. Choi, *Bioresour. Technol.*, **150**, 359 (2013).
  29. A. V. Bridgwater, *Biomass Bioenergy*, **38**, 68 (2012).
  30. M. Ayllón, M. Aznar, J. L. Sánchez, G. Gea and J. Arauzo, *Chem. Eng. J.*, **121**, 85 (2006).
  31. P. Weerachanchai, C. Tangsathitkulchai and M. Tangsathitkulchai, *Korean J. Chem. Eng.*, **28**, 2262 (2011).
  32. R. Maggi and B. Delmon, *Fuel*, **73**, 671 (1994).
  33. J. W. Choi, J. H. Choi, D. J. Suh and H. Kim, *J. Anal. Appl. Pyrol.*, **112**, 141 (2015).
  34. Q. Lu, W. Z. Li and X. F. Zhu, *Energy Convers. Manage.*, **50**, 1376 (2009).
  35. A. Oasmaa and S. Czernik, *Energy Fuels*, **13**, 914 (1999).
  36. D. Chiaramonti, A. Oasmaa and Y. Solantausta, *Renew. Sust. Energy Rev.*, **11**, 1056 (2007).
  37. J. Lehto, A. Oasmaa, Y. Solantausta, M. Kytö and D. Chiaramonti, *Appl. Energy*, **116**, 178 (2014).
  38. J. L. Zheng and Q. Wei, *Biomass Bioenergy*, **35**, 1804 (2011).
  39. S. Czernik and A. V. Bridgwater, *Energy Fuel*, **18**, 590 (2004).
  40. M. J. Antal and M. Grønli, *Ind. Eng. Chem. Res.*, **42**, 1619 (2003).
  41. M. I. Bird, C. M. Wurster, P. H. de Paula Silva, A. M. Bass and R. de Nys, *Bioresour. Technol.*, **102**, 1886 (2011).
  42. L. Beesley, E. Moreno-Jiménez, J. L. Gomez-Eyles, E. Harris, B. Robinson and T. Sizmur, *Environ. Pollut.*, **159**, 3269 (2011).
  43. X. Zhang, H. Wang, L. He, K. Lu, A. Sarmah, J. Li, N. S. Bolan, J. Pei and H. Huang, *Environ. Sci. Pollut. Res.*, **20**, 8472 (2013).
  44. J. Lehmann, *Nature*, **447**, 143 (2007).